



HAL
open science

The taxonomic challenge posed by the Antarctic echinoids *Abatus bidens* and *Abatus cavernosus* (Schizasteridae, Echinoidea).

Bruno David, Thomas Saucède, Anne Chenuil, Emilie Steimetz, Chantal de Ridder

► To cite this version:

Bruno David, Thomas Saucède, Anne Chenuil, Emilie Steimetz, Chantal de Ridder. The taxonomic challenge posed by the Antarctic echinoids *Abatus bidens* and *Abatus cavernosus* (Schizasteridae, Echinoidea).. *Polar Biology*, 2016, 39 (5), pp.897-912. 10.1007/s00300-015-1842-5 . hal-01310170

HAL Id: hal-01310170

<https://hal.science/hal-01310170>

Submitted on 23 Feb 2024

HAL is a multi-disciplinary open access archive for the deposit and dissemination of scientific research documents, whether they are published or not. The documents may come from teaching and research institutions in France or abroad, or from public or private research centers.

L'archive ouverte pluridisciplinaire **HAL**, est destinée au dépôt et à la diffusion de documents scientifiques de niveau recherche, publiés ou non, émanant des établissements d'enseignement et de recherche français ou étrangers, des laboratoires publics ou privés.

41
42
43
44
45
46
47
48
49
50
51
52
53
54
55
56
57
58
59
60
61
62
63
64
65
66
67
68
69
70
71
72
73
74
75
76
77
78
79
80

Introduction

For two decades, cryptic species have been repeatedly described among the Antarctic fauna, challenging the former, classic biogeographic model of Antarctic species with wide, circumpolar distributions (De Broyer et al. 2011; Dettai et al. 2011). The richness and spatial distribution of the Antarctic fauna have been revisited and the underpinning evolutionary processes re-assessed (Kaiser et al. 2013). The occurrence of cryptic species in the Southern Ocean, and on the Antarctic continental shelf in particular was highlighted in many studies of population genetics, in some cases even signing the existence of species flocks (Lecointre et al. 2013). Cryptic species have been described in various Antarctic groups: polychaetes (Schüller 2011), gastropods (Wilson et al. 2013), bivalves (Linse et al. 2007), crustaceans (Held and Wägele 2005; Raupach and Wägele 2006), pycnogonids (Krabbe et al. 2009), cephalopods (Allcock et al. 2010), crinoids (Wilson et al. 2007; Hemery et al. 2012), holothuroids (O'Loughlin et al. 2011), and fish (Smith et al. 2011). Whatever the clade considered, depending on historical and environmental contingencies, the processes leading to cryptic speciation can be related to spatial isolation, disruptive selection, and ecological divergence. Cryptic species being recurrently described in various Antarctic clades, its origin must be sought for in mechanisms impacting the entire Antarctic fauna and linked to relatively fast landscape dynamics that is, rapid alternation between allopatry and sympatry (Aguilée et al. 2012). A common explanation resides in the alternation between glacial and interglacial periods that forces populations to isolated, glacial refugia or otherwise allows species to expand their spatial ranges (Thatje et al. 2005; Allcock and Strugnell 2012; Aguilée et al. 2012).

Unexpectedly, no cryptic species had been so far recorded among Antarctic echinoids, which are, however, relatively well-diversified in the Southern Ocean (Saucède et al. 2014). Spatangoid irregular echinoids in particular form the most speciose group of echinoids in the Southern Ocean. It is exclusively represented there by the family Schizasteridae and counts 30 morphologically recognized species and eight genera (David et al. 2005a, b; Pierrat et al. 2012, Saucède et al. 2014). Most species are brooders, the females incubating their young in deepened petals that form kind of pouches or marsupia. Such a life history trait implies limited dispersal capabilities that might have facilitated this outstanding diversification of the group also promoted by the alternation between glacial and interglacial periods and the flow of the Antarctic Circumpolar Current (Poulin et al. 2002; Pearse et al. 2009). All Antarctic species of Schizasteridae constitute a single monophyletic grouping, which presumably represent a species “core flock” (*sensu* Lecointre et al. 2013) endemic to the Antarctic continental shelf including its deepest parts (David et al. 2005a; Pearse et al. 2009; Lecointre et al. 2013; Saucède et al. 2014). Schizasterids are deposit feeders and soft-bottom dwellers, they live more or less buried into the superficial layer of sediments.

The systematics of Antarctic Schizasteridae has long been explored based on morphological observations (e.g. Mortensen 1909, 1910; Koehler 1912; Pawson 1969; David et al. 2005a, b for the most recent reviews) but several species are known by few specimens and still remain poorly described. Considering the significant variation of morphological characters such as test outline and plating, development and position of fasciolar bands and of other appendages, the taxonomy of Antarctic Schizasteridae and the phylogenetic relationships among species remain puzzling, pending for new appraisals grounded on molecular markers. The R/V *Polarstern* cruise PS81 - ANT XXIX/3 (Gutt 2013) came across populations of *Abatus bidens*, a schizasterid so far known by few specimens that were found living in sympatry with the species *Abatus cavernosus*. The species were formerly considered as two

81 varieties of a same species (Mortensen 1951) before they were placed in two distinct entities (David et al. 2005a). The
82 species *A. cavernosus* is so far reported to have a circum-antarctic distribution, while *A. bidens* is only recorded with
83 certainty in South Georgia and at the northern tip of the Antarctic Peninsula. The later species was also reported in
84 Adelie Land where its occurrence remains uncertain (David et al. 2005a). The present study makes possible to fully
85 describe the species *A. bidens* for the first time and to assess morphological and genetic variations between the two
86 forms. What are the morphological and genetic differences between *A. bidens* and *A. cavernosus* ? Are there reliable,
87 genetic differences to support the distinction between the two nominal species ? Are there transitional forms to
88 suggest that they are cryptic species if any?

89

90 **Materials and methods**

91

92 *Material studied*

93 Seventy nine specimens of *A. bidens* and *A. cavernosus* were collected at 19 stations in the northwest of the Weddell
94 Sea, in the Bransfield Strait, and in the Drake Passage during cruise PS81 of the R/V *Polarstern* (Fig. 1; Table 1).
95 Specimens were collected between 102 and 782 m depth using an Agassiz trawl (Gutt 2013). The two species were
96 found in sympatry at five of the 19 stations. Specimens were subsequently fixed in 96% ethanol and are now housed
97 in collections of the University of Burgundy (Dijon, France). Taxonomy of Antarctic species of the family
98 Schizasteridae is really challenging as shown for long by previous studies (David et al. 2005a, Saucède et al. 2014).
99 We therefore concentrated our study on recently sampled specimens during cruise PS81, for which a special care was
100 taken to control sample preservation, morphological study, and taxonomic identification. Genetic and morphometric
101 analyses were performed independently.

102

103 *Genetic analyses*

104 Genetic analyses initially included 62 specimens among which 49 provided informative sequences to be analyzed.
105 Tissue samples were taken on echinoid spines and DNA was extracted using the Chelex method following Chenuil
106 and Féral (2003). A typical barcoding region of the mitochondrial cytochrome oxidase gene was amplified by PCR
107 using the primers COIe3 (5'- GCTCGTGC(A/G)TCTAC(A/G)TCCAT -3') and COIe5 (5'-
108 GC(C/T)TGAGC(A/T)GGCATGGTAGG -3') from Stockley et al. (2005). PCR amplicons were sent to the industry
109 (Eurofins Genomics) for Sanger sequencing. DNA sequences were manually trimmed and checked using the program
110 Bioedit (Hall 1999). Haplotype networks were built by the median-joining method using the Network software
111 (Bandelt et al. 1999). A color code was used to identify the morphological species, the distribution area (inside the
112 Weddell Sea, the Bransfield Strait, and the Drake Passage), and the sampling stations of each haplotype owing to the
113 NetworkPublisher software (Bandelt et al. 1999).

114

115 *Morphological analyses*

116 Echinoids were observed under a binocular microscope and morphology was analyzed using 10 quantitative
117 parameters measured on echinoid tests with a digital caliper to the nearest 0.1 mm. These measurements were defined
118 based on the morphological characters described in diagnoses of Antarctic echinoid species (David et al. 2005a). They
119 are total test length (LL), total test width (WD), total test height (HT), distance between the apical system and the
120 back of the test (AS), length of posterior petal I (PPT), length of anterior petal II (APT), distance between center of

121 the apical system and beginning of petal II (DP), distance between the periproct and the base of the test (PP), distance
122 between the peristome and the back of the test (PS), and total number of adjacent ambulacral plates abutting the
123 labrum (LB) (Fig. 2). Echinoid size was estimated using the geometric mean of test length, width and height (i.e., the
124 cube root of their product) and test shape (i.e., test proportions) was analyzed using seven indices computed from
125 ratios between some of the 10 measured quantitative parameters: shape at the ambitus ($AMB=WD/LL$), gibbosity
126 ($GIB=HT/[\sqrt{(LL.WD)}]$), relative position of the peristome ($RPS=PS/LL$), relative position of the periproct
127 ($RPP=PP/HT$), relative position of the apical system ($RAS=AS/LL$), relative size of the petals ($RPET=PPT/APT$),
128 relative importance of the gap between the apical system and the beginning of petal II ($RDP=DP/APT$).
129 Morphometric analyses were performed on 75 specimens, 57 identified as *A. bidens* and 18 as *A. cavernosus*, using
130 the softwares Past (Hammer et al. 2001) and Statistica 6.1 (Statsoft 2002). Principal component analyses (PCAs) were
131 performed independently on the 10 quantitative parameters and on the seven indices to analyze morphological
132 variations within and between the two species. Correlation matrices were used to compute the PCAs as raw data show
133 contrasting units and range variations. Morphological differentiation between the two species was analyzed using
134 discriminant analyses based on quantitative measurements and on the indices independently. A priori groups were
135 determined based on genetic data (see below). These analyses were complemented by parametric tests as
136 homoscedasticity assumptions are respected (only parameters PP and LB and indices RPS and RPP show significantly
137 different variances between the two species).

138

139 Appendages were prepared and examined following David and Mooi (1990). Pedicellariae were removed from
140 tests and placed into 96 % ethanol. They were bleached with a 10 % solution of sodium hypochlorite to remove soft
141 tissue and to separate the valves. Then, they were washed in water, dried for 24 h, and mounted on SEM stubs. Details
142 of pedicellariae were examined with a tabletop scanning electron microscope, and digital images were recorded.

143

144 **Results**

145

146 *Genetic analyses*

147 After trimming, the alignment file contained 633 homologous base pairs for 49 individuals. Seven haplotypes were
148 identified and form three divergent haplogroups, each group including two or three haplotypes (Fig. 3). Haplogroups
149 G1 (26 specimens) and G2 (18 specimens) are composed of specimens of *A. bidens* and are separated from one
150 another by a minimum of 17 mutations (i.e., 2.7% of genetic difference). The third haplogroup G3 (5 specimens) is
151 composed of specimens of *A. cavernosus* only, and is separated from haplogroups G1 and G2 by a minimum of 31
152 and 23 mutations respectively (i.e., 5% and 3.5% of genetic difference) (Fig. 3a). Haplogroups were identified at 11 of
153 the 19 sampling stations. Haplogroup G3 was identified at stations of the Drake Passage and in the Bransfield Strait,
154 while the two divergent haplogroups of *A. bidens* were found at stations of the Weddell Sea and of the Bransfield
155 Strait (Fig 3b). The three haplogroups occur in sympatry at two stations only (Sts. 220-2 and 224-3), the two
156 haplogroups of *A. bidens*, G1 and G2, are present together in 3 other stations (Sts. 164-4, 204-2, and 227-2), one
157 single haplotype was identified at the six remaining stations (Fig. 3c).

158

159 *Morphological analyses*

160 Within the 75 specimens measured, 41 were identified as *A. bidens* by genetic analyses, 26 belong to haplogroup G1,
161 15 to haplogroup G2, and 5 more specimens were identified as *A. cavernosus* and belong to haplogroup G3. A total of
162 29 specimens could not be analyzed for genetics and were finally attributed to their respective species based on
163 morphological results that is, 16 specimens to *A. bidens* and 13 to *A. cavernosus*. The distribution of specimens is
164 detailed in Table 1.

165 Statistical analyses of morphological data allow to clearly differentiate the two morphological species *A.*
166 *bidens* and *A. cavernosus*. Five parameters, in particular, were tested significantly different between the two species
167 (Student bilateral tests are detailed in Table 2): the distance between the peristome and the back of the test (PS), the
168 distance between the apical system and the back of the test (AS), the length of the posterior petal I (PPT), the distance
169 between the center of the apical system and the beginning of petal II (DP), and the total number of adjacent
170 ambulacral plates abutting the labrum (LB). Size was not tested significant between the two species (bilateral t-test
171 under homoscedasticity: $p=0.47$) so that morphological differences between species are not due to allometry. Sexual
172 dimorphism was not tested significant either for shape differences (Hotelling's T-squared: $p=0.19$ and $p=0.29$ for raw
173 parameters and shape indices respectively). Size only differs between females and males, females being larger than
174 males (unilateral t-test: $p=0.014$, mean size of females and males: 38.5 mm and 35.4 mm respectively).

175 The principal component analysis performed on the 10 quantitative parameters (Fig. 4) shows that the two
176 species mainly differentiate from one another along PC2 (14.2% of the total variance), which is mainly due to three
177 parameters: labrum extension (LB), length of posterior petal I (PPT), and position of the apical system (AS). The
178 principal component analysis performed on shape indices gave congruent results with a clear differentiation of the two
179 species along the two first PCs (62.9% of the total variance). Differentiation mainly concerns three indices: the shape
180 of the ambitus (AMB), the relative position of the apical system (RAS) and the posterior/ anterior ratio between petals
181 (RPET). Congruent results of the two PCAs show that specimens of *A. bidens* have a more extended labrum, a more
182 elongated ambitus, a more anterior apical system and a longer posterior petal than specimens of *A. cavernosus*. This
183 morphological difference is also supported by the discriminant analyses performed on raw parameters and shape
184 indices, with a high attribution ratio of 98.7% for both parameters and indices (Hotelling's T-squared: $p=9.3 \cdot 10^{-15}$ and
185 $p=2.3 \cdot 10^{-19}$ respectively).

186 Morphological variations between the two genetic groups of *A. bidens*, G1 and G2, were also analyzed. No
187 conspicuous difference was noticed between the two groups when specimens were observed at the naked eye and
188 under the binocular microscope, but statistical analyses revealed significant differences for three following
189 parameters: test height (HT), labrum extension (LB), and distance between the apical system and the beginning of
190 petal II (DP) (Table 3). Variation ranges, however, widely overlap and clear, diagnostic morphological characters
191 cannot be identified to differentiate the two groups. These results are also supported by the PCAs performed on raw
192 parameters (Fig. 5) and shape indices independently. The PCA of raw parameters shows no clear differentiation
193 between morphologies of the two groups along the first two PCs (Fig. 5a), the two groups best differentiating along
194 PC3, which only accounts for 9.35% of the total variance, though widely overlapping with one another (Fig. 5b).
195 These results are congruent with those of the discriminant analyses (Hotelling's T-squared: $p=1.6 \cdot 10^{-5}$ and $p=0.005$ for
196 raw parameters and shape indices respectively), the two groups best differentiating for raw parameters. This
197 discriminant analysis performed on raw parameters also shows that the two groups of *A. bidens* partly overlap with
198 one another in morphology but clearly differentiate from *A. cavernosus* (Fig. 6).

199 Morphological comparison of the three haplotypes demonstrates that they all differ significantly from each
200 other in some of the measured, raw parameters. Pairwise Mahalanobis distances between the three groups were all
201 tested significant regarding raw parameters, while for shape indices only the Mahalanobis distance between G1 and
202 G2 is not significant (Table 4). Haplogroup G1 turns out to be the most different from G3 in morphology, while G2 is
203 intermediate in position. This totally agrees with genetic results, the distance between G1 and G3 being the longest as
204 well (Fig. 3a).

205
206 Besides morphometric analyses, qualitative characters were also examined to complement the morphological
207 study, including observation of appendages (Table 5; Fig. 7). Some characters appear clearly diagnostic of *A.*
208 *cavernosus* and allow to differentiate it from *A. bidens*. In contrast, no single character allows to differentiate the two
209 groups of *A. bidens* from one another.

210 The test outline is heart-shaped in *A. cavernosus*, it is angular with a truncated posterior end in *A. bidens*. The
211 width/length ratio is significantly different between the two species, *A. bidens* being the most elongated (unilateral t
212 test on AMB: $p=2.16 \cdot 10^{-6}$). All petals are almost of the same size in *A. bidens* (mean posterior petals size reaches 93%
213 of that of anterior ones), while posterior petals are shorter in *A. cavernosus* (mean ratio = 64%). The color of test and
214 spines is light brown in *A. bidens*, darker in *A. cavernosus*. The fasciolar band appears beige in *A. bidens*, in which it
215 passes very low anteriorly, and dark purple in *A. cavernosus*. The apical system is anterior in position in *A. bidens*,
216 centered in *A. cavernosus* (it is situated at 39% and 51% of total test length in *A. bidens* and *A. cavernosus*
217 respectively).

218 Regarding plate patterns, in *A. cavernosus* the labrum is short and does not extend farther than the 1st,
219 infrequently the 2nd adjacent ambulacral plate, while in *A. bidens* the labrum extends as far as the 3rd adjoining
220 ambulacral plate, more rarely the 2nd and very seldom the 1st one. Marsupia about the apical system in *A. cavernosus*,
221 what is the most frequent pattern showed by Antarctic brooding schizasterids, while they often do not start before
222 plates 8 or 9 in anterior petals of *A. bidens*, and plates 5 or 6 in the posterior ones (Fig. 8).

223 Pedicellariae of the two species were observed in details (Fig. 7). Globiferous pedicellariae are drastically
224 distinct between the two species. They are not very numerous in *A. cavernosus*, appear black in living specimens
225 when not cleaned of their soft tissue, and valves terminate in a series of four (rarely three) sharp, tiny teeth that are
226 rooted on the upper margin of a circular opening (Fig. 7a). In *A. bidens*, globiferous pedicellariae are extremely
227 numerous on the apical side, they are embedded in white tissue in living specimens, which turns dark in the specimens
228 fixed in ethanol. Valves terminate in two to three very long hooks (Fig. 7d). Rostrate pedicellariae of the two species
229 are relatively similar in shape except for the presence of a narrow, spiky distal tip in *A. bidens* (Fig. 7f), while it is
230 blunt and serrated in *A. cavernosus* (Fig. 7b). Tridentate pedicellariae belong to two main types: (1) the classic type
231 with a spoon-shaped distal part that tappers progressively toward the base and (2) a shovel-shaped type with the distal
232 part separated from the base by a more or less straight shaft (Fig. 7c, e). Both types are present in the two species, but
233 they are more elongated in *A. cavernosus* (Fig. 7c) than in *A. bidens* (Fig. 7e).

234 Sphaeridae are somehow rounded in *A. cavernosus* (Fig. 7g), more elongated in *A. bidens* (Fig. 7h).

235 236 Systematics

237 The systematics and taxonomy of *A. bidens* is revised below based on the new genetic and morphological results
238 obtained in the present work. All results are congruent and show that *A. bidens* should be regarded as a distinct

239 species, following David et al. (2005a), and not a variety (sub-species) of *A. cavernosus*, contrary to Mortensen
240 (1951) and Kroh (2015). The description includes the two haplogroups of *A. bidens* identified in this study, G1 and
241 G2, herein treated as two putative cryptic species. All the specimens figured and studied in the present work are
242 housed in collections of the University of Burgundy, Dijon (France).

243

244 ***Abatus bidens* Mortensen 1910**

245 Figures 7 and 8

246

247 *Abatus cavernosus* var. *bidens* Mortensen, 1910; p. 73; Pl. 19: 32, 35, 39, 42.

248 *Abatus cavernosus* var. *bidens* Mortensen, 1951; p. 256.

249 Non *Abatus bidens* Bernasconi, 1953; p. 44; Pl. 24: 1–6; Pl. 25: 1–4.

250 *Abatus bidens* David et al., 2005a: 190–191.

251 *Abatus cavernosus bidens* Kroh, 2015: <http://www.marinespecies.org/ophiuroida/aphia.php?p=taxdetails&id=513701>

252 *Abatus bidens* Kroh, 2015: <http://www.marinespecies.org/ophiuroida/aphia.php?p=taxdetails&id=160761>

253

254 **Material:** see Table 1 for location of material examined.

255

256 **Diagnosis (Table 5):** apical system anterior in position. Anterior and posterior petals of equal length. Anterior branch
257 of the fasciole low on the test. Labrum extending posteriorly to the 2nd or 3rd adjacent ambulacral plate. Globiferous
258 pedicellariae very numerous on the apical side, particularly between petals and on the two margins of the anterior
259 ambulacrum, with valves terminating in two or three long hooks positioned at the end of a narrow, elongated aperture
260 (Fig. 7d). Living specimens yellow with whitish globiferous pedicellariae.

261

262 **Description**

263 General morphology and plate pattern.

264 Size: The mean length of adult specimens is 46.7 mm, the females being slightly larger than males (unilateral t
265 test: $p=0.008$).

266 Color: Living specimens beige to light brown, sometimes almost yellow (Fig. 8). The color of spines is light
267 beige. The fasciole is of the same color, turning dark in dry specimens. Plate pattern of the apical side is more or less
268 shown by subtle changes in coloration.

269 Outline of the test: Ambitus anteriorly rounded with a faint frontal notch and somehow posteriorly truncated,
270 making an angle covered with a tuft of spines on each side. Test width is 89% to 98% of test length (94% on average).
271 The posterior end of the test is vertically truncated, otherwise dome-shaped. Test height is 60% of test length.
272 Posterior petals are slightly shorter than anterior ones and converge at a more acute angle than anterior ones.

273 Apical system: It is slightly anterior in position, at 39% of the total test length from the anterior. Plating
274 follows the classic *Abatus* ethmolytic pattern with three gonopores (there is no gonopore in genital plate 2).
275 Gonopores larger in females.

276 Periproct: Located on the vertical posterior side, its adoral margin situated at 42% of test height from the lower
277 surface. It is scarcely visible in either apical or oral views. It is embedded between interambulacral plates 5.a.4/5.b.5
278 or 5.a.5/5.b.6 adorally, and 5.a.7/5.b.7 or 5.a.7/5.b.8 apically.

279 Peristome: It is relatively large and discernible as the anterior part of the labrum does not overhang over it. It is
280 anterior in position, located at 31% of test length from the anterior of the test.

281 Plastron: In interambulacrum 5, the labrum is long, extending backward to the 3rd or 2nd adjacent ambulacral
282 plates (sometimes the 4th).

283 Marsupiae (petals) and sexual dimorphism: Anterior and posterior petals almost of the same size, especially in
284 haplogroup G1 (mean ratio = 0.97) compared to haplogroup G2 (mean ratio = 0.87). In most specimens, the adapical
285 extremity of brood pouches is distant from the apical system, a morphological feature diagnostic of *A. bidens*. It is
286 particularly conspicuous in females, in which anterior pouches initiate as far as the 8th to 9th ambulacral plates, while
287 posterior ones are less distant from the apical system. This character is reminiscent of the plate pattern observed in
288 *Abatus nimrodi*.

289 Fasciole: The peripetalous orthofasciole (*sensu* Néraudeau et al. 1998) is very conspicuous and form a broad
290 band of 7 to over 15 rows of miliaries, depending on the segment considered and on test size. The fasciole is excentric
291 anteriorly with the posterior segment distant from the posterior end of the test, and the anterior segment passing very
292 close to the ambitus, barely visible in apical view.

293

294 Appendages

295 Primary spines: They are relatively coarse and of the usual schizasterid shape with finely serrated longitudinal
296 ridges. The largest spines occur on the adoral side, in the plastronal and other interambulacral areas, and are used for
297 locomotion. Their distal extremity is gently curved. The smallest spines are on the apical side and show rounded tips.

298 Secondary spines: Those observed on specimens collected at station 163-9 (Weddell Sea) are club-shaped and
299 densely distributed.

300 Miliaries: They are made of a relatively loose stereom meshwork composed of 7 to 8 longitudinal ridges
301 separated by large openings. They end in a swollen serrated tip.

302 Clavulae: They are straight, made of fenestrated stereom, and end in a tuft of trabeculae. They are very similar
303 in *A. bidens* and *A. cavernosus*.

304 Pedicellariae: The globiferous pedicellariae are extremely numerous, particularly on the apical side in the
305 vicinity of petals and along each side of ambulacrum III. In living specimens, they appear as vivid yellow or whitish
306 spots; they are brownish in specimens preserved in ethanol. Their valves terminate in two or three long hooks located
307 at the top of an elongated opening (Fig. 7d). This character is shared with several other species of *Abatus* (e.g. *A.*
308 *curvidens*, *A. agassizi*, and *A. elongatus*) and can putatively be regarded as plesiomorphic as it is also present in
309 several species of *Amphipneustes* and *Tripylus*.

310 Tridentate pedicellariae (dentate pedicellariae are very commonly tridentate, sometimes bidentate) belong to
311 two main types. As indicated above, valves of type 1 have a spoon-shaped distal part that tappers progressively
312 toward the base (Fig. 7e). Valves of type 2 comprise three parts: the base, the intermediary tubular part, and the
313 spoon-shaped, and finely serrated distal part (Fig. 7e). Rostrate pedicellariae display a very long and curved blade
314 with small lateral teeth along the rim of the blade (Fig. 7f).

315 Sphaeridia: They are slightly ovoid and ornamented with small meridian ridges and grooves (Fig. 7h).

316

317 **Distribution:** *A. bidens* was reported with confidence by the Swedish South Polar and Discovery expeditions from
318 the South Georgia Islands, between 64 and 270 m (Mortensen 1910), and along the Antarctic Peninsula in the
319 Bransfield Strait and in the northwest of the Weddell Sea, between 102 and 782 m (this study).

320

321 **Remarks:** Mortensen (1951) regarded *A. bidens* as a subspecies of *A. cavernosus* but suggested that it could be a
322 distinct species. David et al. (2005a) considered *A. bidens* as a separate species because globiferous pedicellariae of
323 the two species are very different. Following Mortensen (1951) and David et al. (2005a), the specimens described by
324 Bernasconi (1953) as *A. bidens* are considered here as representatives of *Tripylus excavatus* because adult individuals
325 possess a conspicuous latero-anal fasciolar branch, absent in *A. bidens*. The two cryptic species (genetic groups G1
326 and G2) are here referred to as *A. bidens* pending for new data.

327

328 **Discussion**

329 In the present study, morphological and genetic results show that the two nominal species *A. cavernosus* and *A. bidens*
330 are clearly distinct and should be regarded as truly different species as formerly suggested by David et al. (2005a).
331 Several morphological features were recognized as clear, diagnostic characters of *A. bidens*, among which the number
332 and shape of globiferous pedicellariae are the most remarkable (Table 5). Other distinctive, and more accessible
333 characters, albeit not so clear cut, are petal relative size (anterior and posterior petals are of the same size in *A. bidens*)
334 and the position of the apical system (anterior in *A. bidens*). These characters are reliable enough for the field
335 determination of the species.

336 Unexpectedly, two genetic groups of *A. bidens* were identified. The genetic divergence between the two groups
337 (2.7%) is significant enough to suggest that they could be reproductively isolated from each other. This is congruent
338 with results obtained with molecule COI for other echinoderms. Genetic distance between closely related species of
339 echinoderms usually ranges between 0.62% and 1.3% (Ward et al. 2008; Hoareau and Boissin 2010). Some cryptic
340 species can even display up to 3% of genetic divergence (Egea et al. 2015). For instance, the most closely related
341 lineages within the species complex *Ophioderma longicauda* display a COI divergence of 2.2% (Boissin et al. 2011),
342 and cryptic species of the sand dollar *Mellita longifissa* show a genetic divergence comprised between 5.60% and
343 3.97% (Coppard et al. 2013). Hence, in the present study, the 2.7% of divergence between haplogroups G1 and G2 of
344 *A. bidens*, the absence of intermediate forms between them, and the short genetic distance between them and *A.*
345 *cavernosus* (3.5% to 5%) strongly suggest that they constitute two cryptic species, all the more as schizasterid
346 echinoids were shown to present slow rates of mitochondrial DNA evolution (Chenuil et al. 2008, 2010). The lack of
347 clear-cut discrimination within morphological variations of the two forms of *A. bidens* is in line with this
348 interpretation. Some morphological differences between the two genetic groups were tested significant but most
349 variations significantly overlap. Three evolutionary scenarios, however, can challenge our interpretation because they
350 too can generate divergent lineages in a biological species with no intermediate forms: a past demographic bottleneck,
351 a selective sweep, and a long-lasting vicariance that did not result in an efficient reproductive barrier before
352 “secondary” contact. The only way to rule these scenarios out and prove that haplogroups G1 and G2 form true
353 cryptic species of *Abatus bidens*, experimental crosses excepted, would consist in characterizing at least one
354 additional genetic marker independent from the mitochondrial COI gene that is, a DNA nuclear marker.

355 The two groups of *A. bidens* were collected in sympatry at the scale of sampling stations (they were found
356 together at five of the eight stations at which they were identified). *A. cavernosus* was found living in sympatry with

357 *A. bidens* at five stations of the 12 stations at which it was collected, and the three haplogroups were found together at
358 four of these stations. Despite the limited number of sampling sites, the occurrence of species together was frequent
359 and attests that they can be living in sympatry. The co-existence of closely related species of similar forms is
360 generally considered a rare phenomenon as sympatry presumes the existence of differences in ecological niches and
361 life history traits. In environments of the Southern Ocean, such cases are known in amphipods (Baird et al. 2011),
362 isopods (Held 2001), and crinoids (Hemery et al. 2012). In irregular echinoids, sympatry was observed between
363 closely related species of the genus *Echinocardium* (between *Echinocardium cordatum* and *Echinocardium flavescens*
364 in Norway, pers. obs.), as well as between species of the sand dollar *Mellita* along the tropical coasts of the Americas
365 (Coppard et al. 2013). Sympatry between attested, cryptic species is much more rare. Examples are documented in the
366 sand dollar *Mellita*, in which only one of nine possible cases of sympatry between cryptic species was recorded
367 (Coppard et al. 2013), and in the species complex *E. cordatum* (Egea et al. 2011; Egea et al. 2015). Contrary to these
368 two case studies, all species of *Abatus* are brooders and consequently, show limited dispersal capability compared to
369 sea urchins with planktonic larvae. The co-existence of *A. bidens* and *A. cavernosus* at the same sites (Fig. 3c) is
370 therefore unexpected, all the more that previous studies revealed significant genetic differentiation between
371 populations of *Abatus* species at small spatial scale such as in *Abatus cordatus* (Poulin and Féral 1995; Ledoux et al.
372 2012), *Abatus agassizi* (Díaz et al. 2012), and *Abatus nimrodi* (Chenuil et al. 2004). In the present case study, the
373 mechanisms involved in the separation between the three forms cannot be uncovered with confidence. Morphological
374 similarities exclude the hypothesis of a strict ecological mechanism at the origin of the divergence for the three
375 groups, and the two forms of *A. bidens* in particular probably have similar modes of life. The separation is more likely
376 rooted in life history traits (e.g. shifts in spawning seasons) or in prezygotic isolation (i.e. incompatibility between
377 gamete recognition proteins) (Lessios 2011). Finally, it cannot be excluded that haplogroups of *A. bidens* may
378 interbreed with no fitness cost and belong to the same biological species, nor that post-zygotic incompatibility only is
379 involved in the isolation of the two forms despite the evolutionary cost it would imply.

380 At the scale of the three geographic areas explored, the two forms of *A. bidens* were not collected in the Drake
381 Passage, while conversely, *A. cavernosus* was frequently found there (at 83% of the sampling sites). The latter species
382 is also present in the Bransfield Strait but it was less frequently found than *A. bidens*, and it is absent from the
383 northwest of the Weddell Sea (namely no sequence of *A. cavernosus* was identified in the Weddell Sea) (Fig. 9). Two
384 distinct distribution patterns seem to appear and to follow reverse, latitudinal gradients: *A. cavernosus* is the most
385 frequently encountered to the north, and most often outside the areas strongly impacted by sea ice, while the two
386 forms of *A. bidens* are the most frequent to the south in areas under sea ice influence (Fig. 9). Though still in need for
387 further research, these apparent patterns are supported by records of *A. cavernosus* at the tip of South America
388 (Bernasconi 1925, 1966) and by the putative presence of *A. bidens* in Adelie Land (Koehler 1926) described
389 globiferous pedicellariae of "*A. cavernosus*" with two long hooks, suggesting that its specimens should be regarded as
390 *A. bidens*). The two species have been also unquestionably recognized to co-occur in South Georgia (Bernasconi
391 1953). This is not contradictory with the proposed pattern as South Georgia has been often regarded as a
392 biogeographic area under the cross influence of Antarctic and sub-Antarctic regions. Although unevenly distributed,
393 the three haplogroups co-occur in the Bransfield Strait where they can be found in sympatry. Such a diversity pattern
394 has already been highlighted in previous studies for other organisms (Wilson et al. 2007; Hemery et al. 2012). Along
395 with the Scotia Arc region and the northern tip of the Antarctic Peninsula, the Bransfield Strait is a favored zone of

396 connectivity among populations due to the strong current systems present near the tip of the Antarctic Peninsula
397 (Thompson et al. 2009).

398 At the scale of the entire Southern Ocean, the attested occurrence of *A. bidens* in the Peninsula area as well as
399 in Adelie Land suggests that the species has a wide, potentially circumpolar distribution. The respective distribution
400 of the two halpogroups still remain to be clarified, in East Antarctica in particular. In contrast, *A. cavernosus* seems to
401 have a more northern distribution, potentially restricted to the Magellanic and Scotia Arc regions as no report of *A.*
402 *cavernosus* outside this area is fully certain. This distribution pattern is in complete opposition with previous works
403 (David et al. 2005a).

404

405 **Conclusion**

406 Pending for further genetic analyses including closely related species of *Abatus* (i.e. *Abatus philippi*, *A. agassizi*, and
407 *A. cordatus*) and additional samplings in other areas of the Southern Ocean, the present study, however, suggests that
408 the *A. cavernosus* - *A. bidens* complex comprises at least two morphologically close species and two cryptic species.
409 It contributes to clarifying the systematics of *A. cavernosus* and *A. bidens* and shows that *A. bidens* should definitely
410 be regarded as distinct from *A. cavernosus*, based on congruent morphological characters and genetic results. In
411 addition, *A. cavernosus* and the two forms of *A. bidens* were shown to have distinct distribution patterns.

412 The present work is also the first study to report the occurrence of cryptic species of echinoids in the Southern
413 Ocean, in accordance with many observations of various marine invertebrates of the Southern Ocean. It leads to
414 revisit the richness of the Antarctic echinoid fauna, its systematics, macroecological patterns, and to re-assess the
415 underpinning evolutionary processes and history. It also highlights the crucial importance of associated morphological
416 and genetic studies for improving our knowledge of Antarctic biodiversity. This is a prerequisite for further process-
417 based studies, from ecology to phylogeography, and for uncovering the origin of the rich Antarctic biodiversity.

418

419 **Acknowledgements**

420 Samples were collected during the oceanographic campaign PS81 - ANT-XXIX/3 of the R/V *Polarstern*. The authors
421 would like to thank Prof. Dr. Julian Gutt, chief scientist of this campaign, as well as the crew and the scientific staff.
422 Chantal De Ridder was supported by F.R.S-FNRS "short stay abroad" travel grants (grant nr. 2013/V3/5/035). This is
423 contribution nr. **XX** to the vERSO project (www.versoproject.be), funded by the Belgian Science Policy Office (BELSPO,
424 contract nr. BR/132/A1/vERSO). This is a contribution to team BioME of the CNRS laboratory Biogéosciences
425 (UMR 6282), and MARE publication nr. **YY**.

426

427

428 **Conflict of interest**

429 The authors declare that they have no conflict of interest.

430

431

432 **References**

433 Aguilée R, Claessen D, Lambert A (2012) Adaptive radiation driven by the interplay of eco-evolutionary and
434 landscape dynamics. *Evolution* 67(5):1291-1306. doi:10.1111/evo.12008

435 Allcock AL, Barratt I, Eléaume M, Linse K, Smith PJ, Steinke G, Stevens DW, Norman MD, Strugnell JM (2010)

436 Cryptic speciation and the circumpolarity debate: A case study on endemic Southern Ocean octopuses using
437 the COI barcode of life. *Deep-Sea Res II* 58:242-249.

438 Allcock AL, Strugnell JM (2012) Southern Ocean diversity: new paradigms from molecular ecology. *Trends Ecol*
439 *Evol* 27:520-528

440 Bandelt HJ, Forster P, Röhl A (1999) Median-joining networks for inferring intraspecific phylogenies. *Mol Biol Evol*
441 16:37-48

442 Bernasconi I (1925) Resultados de la primera expedicion a Tierra del Fuego (1921). Echinodermos. I Equinoideos.
443 *Anales Soc Ci Argent* 98:3-17

444 Bernasconi I (1953) Monografia de los equinoideos argentinos. *Anales Mus Nac Hist Nat Buenos Aires* 2(6):1-58

445 Bernasconi I (1966) Los equinoideos y asteroideos colectados por el buque oceanografico R/V "Vema", frente a las
446 costas argentinas, uruguayas y sur de Chile. *Revista Mus Argent Ci Nat "Bernardino Rivadavia"* 9:147-175

447 Coppard S, Zigler KS, Lessios HA (2013) Phylogeography of the sand dollar genus *Mellita*: Cryptic speciation along
448 the coasts of the Americas. *Mol Phylogenet Evol* 69:1033-1042

449 Boissin E, Stöhr S, Chenuil A (2011) Did vicariance and adaptation drive cryptic speciation and evolution of brooding
450 in *Ophioderma longicauda* (Echinodermata: Ophiuroidea), a common atlanto-mediterranean ophiuroid? *Mol*
451 *Ecol* 20:4737-4755

452 Chenuil A, Gault A, Féral JP (2004) Paternity analysis in the Antarctic brooding sea urchin *Abatus nimrodi*. A pilot
453 study. *Polar Biol* 27:117-182

454 Chenuil A, Egea E, Rocher C, Touzet H, Féral JP (2008) Does hybridization increase evolutionary rates ? Data from
455 the 28S-rDNA D8 domain in echinoderms. *J Mol Evol* 67:539–550

456 Chenuil A, Féral JP (2003) Sequences of mitochondrial DNA suggest that *Echinocardium cordatum* is a complex of
457 several sympatric or hybridizing species. A pilot study. In: Féral JP & David B (eds) *Echinoderm Research*
458 2001, Swets & Zeitlinger, Lisse, pp 15-21

459 Chenuil A, Egea E, Rocher C, Féral JP (2010) Comparing substitution rates in spatangoid sea urchins with putatively
460 different effective sizes, and other echinoderm datasets. In: Harris LG, Böttger SA, Walker CW, Lesser MP
461 (eds) *Echinoderms* Durham, Balkema, Leiden, pp 159-161

462 David B, Choné T, Mooi R, De Ridder C (2005a) Antarctic Echinoidea. *Synopses of the Antarctic Benthos*. Koeltz
463 Scientific Books, Königstein

464 David B, Choné T, Mooi R, De Ridder C (2005b) Biodiversity of Antarctic echinoids: a comprehensive and
465 interactive database. *Sci Mar* 69:201–203

466 De Broyer C, Danis B et al (2011) How many species in the Southern Ocean? Towards a dynamic inventory of the
467 antarctic marine species. *Deep-Sea Res II* 58:5-17

468 Dettai A, Adamowicz SJ, Allcock L, Arango CP, Barnes DKA, Barratt I, Chenuil A, Coulloux A et al (2011) DNA
469 Barcoding and molecular systematics of the benthic and demersal organisms of the CEAMARC survey.
470 *Polar Science* 5:298–312

471 Díaz A, González-Wevar CA, Maturana CA, Palma AT, Poulin E, Gérard K (2012) Restricted geographic distribution
472 and low genetic diversity of the brooding sea urchin *Abatus agassizii* (Spatangoidea: Schizasteridae) in the
473 South Shetland Islands: a bridgehead population before the spread to the northern Antarctic Peninsula. *Rev*
474 *Chil Hist Nat* 85:457-468

475 Egea E, David B, Choné T, Laurin B, Féral JP, Chenuil A (2015) Morphological and genetic analyses reveal a cryptic
476 species complex in the echinoid *Echinocardium cordatum* and rule out a stabilizing selection explanation. Mol
477 Phylogenet Evol. doi:10.1016/j.ympev.2015.07.023

478 Egea E, Mérigot B, Mahé-Bézac C, Féral JP, Chenuil A (2011) Differential reproductive timing in *Echinocardium*
479 *spp.*: the first Mediterranean survey allows inter-oceanic and inter-specific comparisons. C R Biol 334:13-23

480 Gutt J (2013) The expedition of the research vessel “Polarstern” to the Antarctic in 2013 (ANT-XXIX/3). Berichte zur
481 Polar- und Meeresforsch 665:1-151

482 Hall TA (1999) BioEdit: a user-friendly biological sequence alignment editor and analysis program for Windows
483 95/98/NT. Nucleic Acids Symp Ser 41:95-98

484 Hammer Ø, Harper DAT, Ryan PD (2001) PAST: Paleontological Statistics Software Package for Education and Data
485 Analysis. Pal Elec 4(1):1-9

486 Held C (2001) No evidence for slow-down of molecular substitution rates at subzero temperatures in Antarctic serolid
487 isopods(Crustacea,Isopoda, Serolidae). Polar Biol 24:497-501

488 Held C, Wägele JW (2005) Cryptic speciation in the giant Antarctic isopod *Glyptonotus antarcticus* (Isopoda:
489 Valvifera: Chaetiliidae). Sci Mar 69(2):175-181

490 Hemery LG, Eléaume M, Roussel V, Améziane N, Gallut C, Steinke D, Cruaud C, Couloux A, Wilson NG (2012)
491 Comprehensive sampling reveals circumpolarity and sympatry in seven mitochondrial lineages of the Southern
492 Ocean crinoid species *Promachocrinus kerguelensis* (Echinodermata). Mol Ecol 21:2502-2518

493 Hoareau TB, Boissin E (2010) Design of phylum-specific hybrid primers for DNA barcoding: addressing the need for
494 efficient COI amplification in the Echinodermata. Mol Ecol Res 10:960–967

495 Kaiser S, Brandão SN, Brix S, Barnes DKA, Bowden DA, David B, Gutt J, et al (2013) Pattern, process and
496 vulnerability of Antarctic and Southern Ocean benthos - a decadal leap in knowledge and understanding. Mar
497 Biol 160:2295-2317

498 Koehler R (1912) Echinodermes nouveaux recueillis dans les mers antarctiques par le Pourquoi-pas (astéries,
499 ophiures et échinides). Zool Anz 39:151-163

500 Koehler R (1926) Echinodermata Echinoidea. In: Australasian Antarctic expedition 1911-1914. Sci Rep (C8):1-
501 134

502 Krabbe K, Leese F, Mayer C, Tollrian R, Held C (2009) Cryptic mitochondrial lineages in the widespread pycnogonid
503 *Colossendeis megalonyx* Hoek, 1881 from Antarctic and Subantarctic waters. Polar Biol 33:281-292

504 Kroh A (2015) *Abatus cavernosus bidens* Mortensen, 1910. In: Kroh A and Mooi R(eds) World Echinoidea Database.
505 Accessed through: World Register of Marine Species

506 Lecointre G, Améziane N, Boisselier MC, Bonillo C, Busson F, Causse R, Chenuil A, Couloux A et al (2013) Is the
507 Species Flock Concept Operational? The Antarctic Shelf Case. PloS ONE 8:e68787

508 Ledoux JB, Tarnowska K, Gérard K, Lhuillier E, Jacquemin B, Veydmann A, Féral JP, Chenuil A (2012) Fine-scale
509 spatial genetic structure in the brooding sea urchin *Abatus cordatus* suggests vulnerability of the Southern
510 Ocean marine invertebrates facing global change. Polar Biol 35:611-623

511 Lessios HA (2011) Speciation genes in free-spawning marine invertebrates. Integr Comp Biol 51:456-465

512 Linse K, Cope T, Lörz AN, Sands C (2007) Is the Scotia Sea a centre of Antarctic marine diversification? Some
513 evidence of cryptic speciation in the circum-Antarctic bivalve *Lissarca notorcadensis* (Arcoidea:
514 Philobryidae). Polar Biol 30:1059-1068

515 Mortensen T (1909) Die Echinoiden der Deutschen Südpolar Expedition 1901-1903. Deutsche Südpolar
516 Expedition. G. Reimer, Berlin

517 Mortensen T (1910) The Echinoidea of the Swedish South Polar Expedition. Wissenschaftliche Ergebnisse der
518 Schwedischen Südpolar-Expedition 1901-03. Lithographisches Institut des Generalstabs, Stockholm

519 Mortensen T (1951) A monograph of the Echinoidea. Vol. 5.2 Spatangoida II. Reitzel CA, Copenhagen

520 Néraudeau D, David B, Madon C (1998) Tuberculation in spatangoid fascioles: Delineating plausible homologies.
521 Lethaia 31:323-334

522 O'Loughlin, PM, Paulay G, Davey N, Michonneau F (2011) The Antarctic region as a marine biodiversity hotspot for
523 echinoderms: diversity and diversification of sea cucumbers. Deep-Sea Res II 58, 264-275

524 Pawson DL (1969) Echinoidea. In: Bushnell VC, Hedgpeth JW (eds) Distribution of selected groups of marine
525 invertebrates in water south of 35° S latitude. Antarctic map folio. Amer Geograph Soc, New York, pp
526 38-41

527 Pearse J, Mooi R, Lockhart SJ, Brandt A (2009) Brooding and Species Diversity in the Southern Ocean: Selection for
528 Brooders or Speciation within Brooding Clades? In: Krupnik I, Lang MA, Miller SE (eds) Smithsonian at the
529 Poles: Contributions to International Polar Year science. Smithsonian Institution Scholarly Press,
530 Washington, pp 181-196

531 Pierrat B, Saucède T, Festeau A, David B (2012) Antarctic, sub-Antarctic and cold temperate echinoid database.
532 ZooKeys 204:47–52. doi:10.3897/zookeys.204.3134

533 Poulin E, Féral J-P (1995) Pattern of spatial distribution of a brood-protecting Schizasterid Echinoid, *Abatus cordatus*,
534 endemic to Kerguelen Islands, Mar Ecol Prog Ser 118:179–186

535 Poulin E, Palma AT, Féral J-P (2002) Evolutionary versus ecological success in Antarctic benthic invertebrates.
536 Trends Ecol Evol 17:218–222

537 Raupach MJ, Wägele JW (2006) Distinguishing cryptic species in Antarctic Asellota (Crustacea: Isopoda) - a
538 preliminary study of mitochondrial DNA in *Acanthaspidia drygalskii*. Antarctic Sci 18:191-198

539 Saucède T, Pierrat B, David B (2014) Chapter 5.26. Echinoids. In: De Broyer C, Koubbi P, Griffiths HJ, Raymond B,
540 d'Udekem d'Acoz C et al (eds) Biogeographic atlas of the Southern Ocean. Scientific Committee on Antarctic
541 Research, Cambridge, pp 213-220

542 Schüller M (2011) Evidence for a role of bathymetry and emergence in speciation in the genus *Glycera* (Glyceridae,
543 Polychaeta) from the deep Eastern Weddell Sea. Polar Biol 34:549-564

544 Smith PJ, Steinke D, McMillan PJ, Stewart AL, McVeagh SM, Diaz de Astarloa JM, Welsford D, Ward RD (2011)
545 DNA barcoding highlights a cryptic species of grenadier *Macrourus* in the Southern Ocean. J Fish Biol
546 78:355-365

547 Statsoft France (2002) STATISTICA (logiciel d'analyse de données). Versio 6, www.Statsoft.com

548 Thatje S, Hillenbrand C, Larter R (2005) On the origin of Antarctic marine benthic community structure. Trends Ecol
549 Evol 20:534-540

550 Thompson AF, Heywood KJ, Thorpe SE, Renner AHH, Trasvina A (2009) Surface circulation at the tip of the
551 Antarctic Peninsula from drifters. J Phys Oceanogr 39:3-26

552 Ward RD, Holmes BH, O'Hara TD (2008) DNA barcoding discriminates echinoderm species. Mol Ecol Res 8:1202-
553 1211

554 Wilson NG, Hunter RL, Lockhart SJ, Halanych KM (2007) Multiple lineages and absence of panmixia in the
555 “circumpolar” crinoid *Promachocrinus kerguelensis* from the Atlantic sector of Antarctica. *Mar Biol* 152:895-
556 904

557 Wilson NG, Maschek A, Baker BJ (2013) A Species Flock Driven by Predation? Secondary Metabolites Support
558 Diversification of Slugs in Antarctica. *PLoS ONE* 8:e80277

559

560 **Figure and table captions**

561

562 **Fig. 1** The 19 stations in the Weddell Sea (yellow dots), Bransfield Strait (orange dots), and Drake Passage (blue dots)
563 where the studied specimens of *Abatus cavernosus* and *Abatus bidens* were collected during cruise PS81 of the R/V
564 *Polarstern*

565

566 **Fig. 2** Measurements performed in the morphometric analysis. a, echinoid test drawn in apical view (fasciolar band in
567 light grey, brood pouches in black, apical system detailed in the center). b, test in posterior view (fasciolar band in
568 light grey, brood pouches and periproct in black). c, test in oral view with details of plate patterns (peristome in
569 black). a, total test length (LL) and width (WD), distance between the apical system and the back of the test (AS),
570 length of posterior petal I (PPT), length of anterior petal II (APT), distance between center of the apical system and
571 beginning of petal (pouch) II (DP). b, total test height (HT), distance between the periproct and the base of the test
572 (PP). c, distance between the peristome and the back of the test (PS); total number of adjacent ambulacral plates
573 abutting the labrum (LB). A maximum of six ambulacral plates (3 per ambulacrum) can abut the labrum in *Abatus*
574 *bidens*; two ambulacral plates only abut the labrum in the specimen drawn in Figure 2c

575

576 **Fig. 3** Median-joining network of haplotypes based on mtDNA COI sequences obtained from 5 specimens of *Abatus*
577 *cavernosus* and 44 specimens of *Abatus bidens*. a, each haplotype is labelled from H1 to H8, and shown in a colored
578 circle indicating the genetic unit to which it belongs: G1 (light green), G2 (dark green), and G3 (red). Size of circles
579 proportional to frequency in the sample analyzed. Mutations shown with unlabelled red dots. Minimum pairwise
580 distances (minimum number of mutations) between specimens of the three groups shown in the table inserted. b,
581 colors indicating the sampling geographic area of each haplotype: the Bransfield Strait (orange), Weddell Sea
582 (yellow), and Drake Passage (blue). c, colors indicating the sampling stations of each haplotype

583

584 **Fig. 4** Principal component analysis of the ten raw morphometric parameters measured in specimens of *Abatus bidens*
585 (green dots) and *Abatus cavernosus* (red dots). The two species differentiate along the first two principal components,
586 which account for 75.06% of the total variance

587

588 **Fig. 5** Principal component analysis of the ten raw morphometric parameters measured in specimens of *Abatus bidens*
589 (G1, light green dots; G2, dark green dots). a, the first two principal components, which account for 78.82% of the total
590 variance. b, first and third principal components, which accounts for 76.53% of the total variance

591

592 **Fig. 6** Discriminant analysis of the ten raw morphometric parameters measured in specimens of *Abatus bidens* (G1,
593 light green dots; G2, dark green dots) and *Abatus cavernosus* (G3, red dots)

594

595 **Fig. 7** Pedicellariae and sphaeridia in *Abatus cavernosus* (a-c, g) and *Abatus bidens* (d-f, h). a, isolated valve of
596 globiferous pedicellaria from specimen UBGD 279061 (G3). b, valves of rostrate pedicellariae from specimens
597 UBGD 279063 (G3), UBGD 279061 (G3), and UBGD 279064 (G3) from left to right. c, valves of tridentate
598 pedicellariae from specimens UBGD 279062 (G3), UBGD 279064 (G3), and UBGD 279063 (G3) from left to right.
599 d, valves of globiferous pedicellariae from specimens UBGD 279067 (G1) and UBGD 279070. e, tridentate
600 pedicellariae from specimen UBGD 279067 (G1). f, rostrate pedicellariae from specimens UBGD 279069 (G1), and
601 UBGD 279070. g, sphaeridia from specimens UBGD 279062 (G3) and UBGD 279064 (G3). h, sphaeridia from
602 specimens UBGD 279070 and UBGD 279068

603

604 **Fig. 8** *Abatus cavernosus* (a-d) and *Abatus bidens* (e-h). a, apical view of fresh specimen UBGD 279059. b, apical, c,
605 oral, and d, posterior views of denuded test of specimen UBGD 279060. e, apical view of fresh specimen UBGD
606 279065. f, apical, g, oral, and h, posterior views of denuded test of specimen UBGD 279066. Scale bars: 10 mm

607

608 **Fig. 9** Distribution map of the genetic groups of *Abatus cavernosus* and *Abatus bidens* (G1, light green; G2, dark
609 green; G3, red) among the 14 stations where they were identified. Circle wedges indicate presence/absence of genetic
610 groups, not abundance

611

612 **Table 1** Sites where specimens of the species complex *Abatus cavernosus* – *Abatus bidens* were collected. Crosses
 613 indicate where the haplogroups were formally identified and where non-sequenced specimens were identified based
 614 on morphology alone.
 615

Sampling sites	<i>Abatus bidens</i>			<i>Abatus cavernosus</i>	
	haplogroup G1	haplogroup G2	non-sequenced	haplogroup G3	non-sequenced
Weddell (162-7)		X			
Weddell (163-9)	X	X			X
Weddell (164-4)	X	X			X
Weddell (188-4)			X		
Weddell (190-2)			X		
Bransfield (116-9)				X	
Bransfield (196-8)			X		
Bransfield (197-5)	X				
Bransfield (198-5)		X			X
Bransfield (199-4)			X		
Bransfield (204-2)	X	X			
Bransfield (205-1)			X		
Bransfield (220-2)	X	X		X	
Bransfield (224-3)	X	X		X	
Bransfield (227-2)	X				
Drake (234-5)				X	
Drake (237-3)					X
Drake (240-3)					X
Drake (245-1)					X

616
 617
 618 **Table 2** Morphological differences between haplogroups of *Abatus bidens* and *Abatus cavernosus*. The table gives the
 619 probability values for Student bilateral tests. Significant values only are detailed (abbreviations are given in Fig. 2)
 620

Parameters	LL, WD, HT, PP, APT	PS	AS	PPT	DP	LB
<i>p</i> values	> 0.05	0.004	1.6 10 ⁻⁷	1.2 10 ⁻⁹	0.015	1.3 10 ⁻⁶

621
 622
 623 **Table 3** Morphological differences between haplogroups G1 and G2 of *Abatus bidens*. The table gives the probability
 624 values for Student bilateral tests. Significant values only are detailed (abbreviations are given in Fig. 2)
 625

Parameters	LL, WD, PS, PP, AS, PPT, APT	HT	DP	LB
<i>p</i> values	> 0.05	0.02	0.01	0.01

626
 17

627
628
629
630
631
632
633

Table 4 Pairwise Mahalanobis distances between haplogroups G1, G2, and G3 of *Abatus bidens* and *Abatus cavernosus* respectively. The table gives the probability values for comparisons using raw variables (matrix upper half) and shape indices (matrix lower half). Asterisks indicate if differences are significant (*) or highly significant (**)

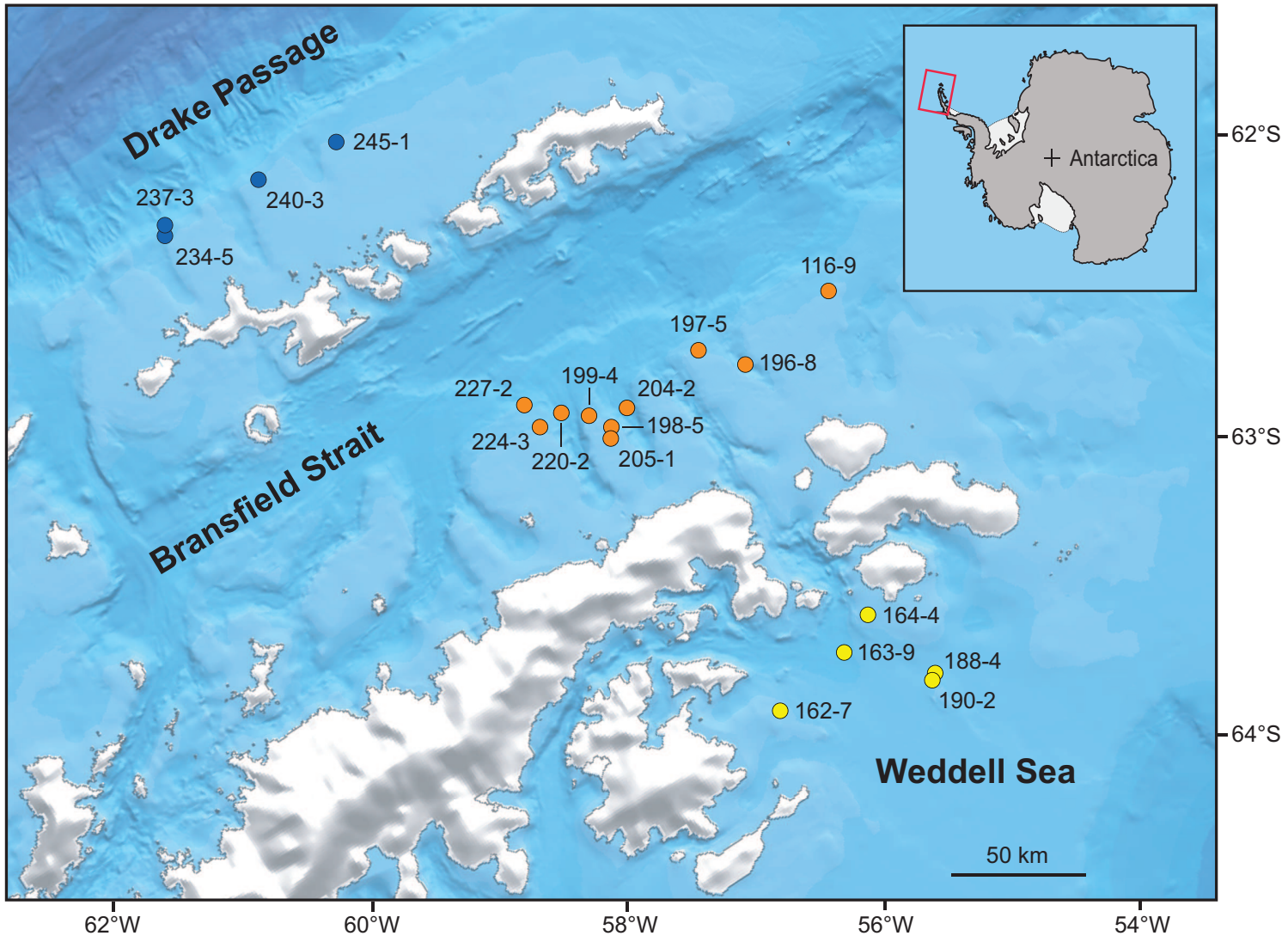
	G1	G2	G3
G1		0.0368*	0.0005**
G2	0.7518		0.0292*
G3	0.0007**	0.0064**	

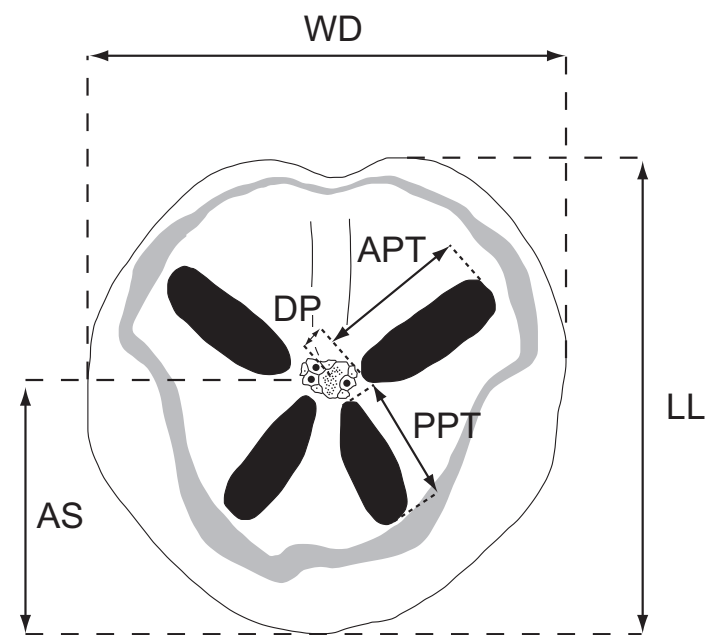
634
635
636
637
638
639

Table 5 Diagnostic morphological characters of *Abatus bidens* (including the two genetic groups) that clearly differ from those of *Abatus cavernosus*. Characters are listed in order of importance for distinguishing the two species

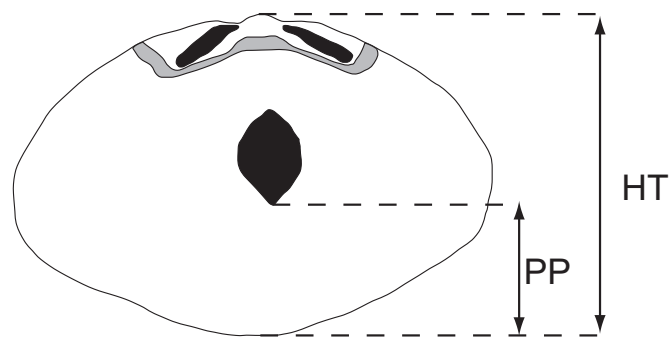
	<i>A. bidens</i>	<i>A. cavernosus</i>
Globiferous pedicellariae	They are numerous, particularly on the apical side. Their valves terminate by two long hooks located above a narrow, elongated aperture.	They are rare. When present, a series of three to four teeth borders the upper rim of a rounded aperture.
Petals	Posterior petals about the same length as the anterior ones.	Posterior petals shorter than the anterior ones.
Color	Living specimens yellow. Globiferous pedicellaria whitish.	Living specimens brownish.
Apical system and fasciole	Shifted anteriorly.	Centered.
Labrum	It extends posteriorly to the 2 nd or 3 rd adjacent ambulacral plates.	It extends posteriorly to the 1 st (or 2 nd) adjacent ambulacral plates.
Brooding pouches (in females)	They often start away from the apical system.	Always starting close to the apical system.
Sphaeridia	Elongated	Rounded or flattened

640

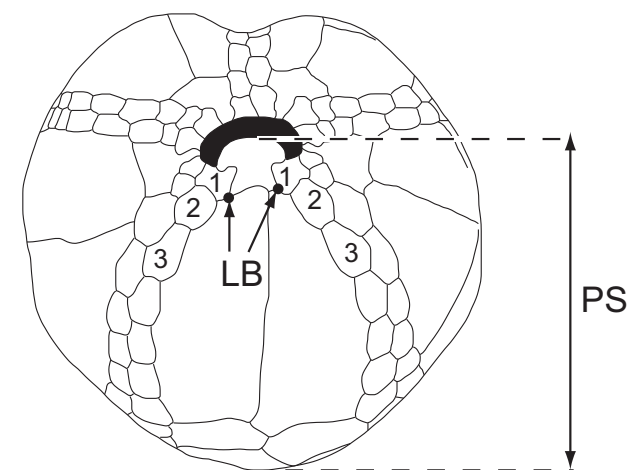




a



b

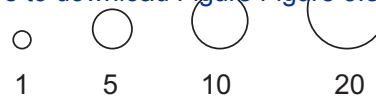


c

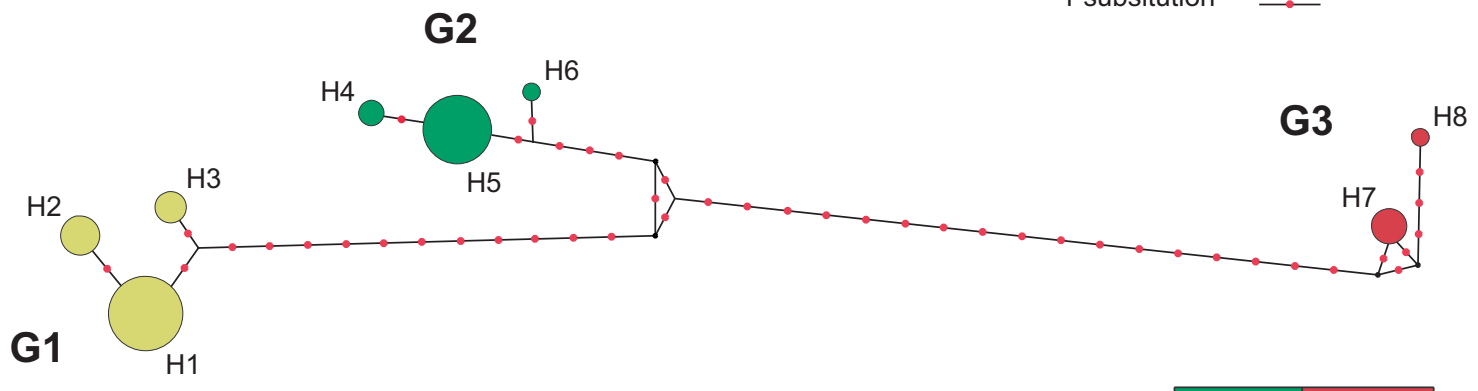
Figure 3 Species

[Click here to download Figure Figure 3.eps](#)

- ● *Abatus bidens*
- *Abatus cavernosus*



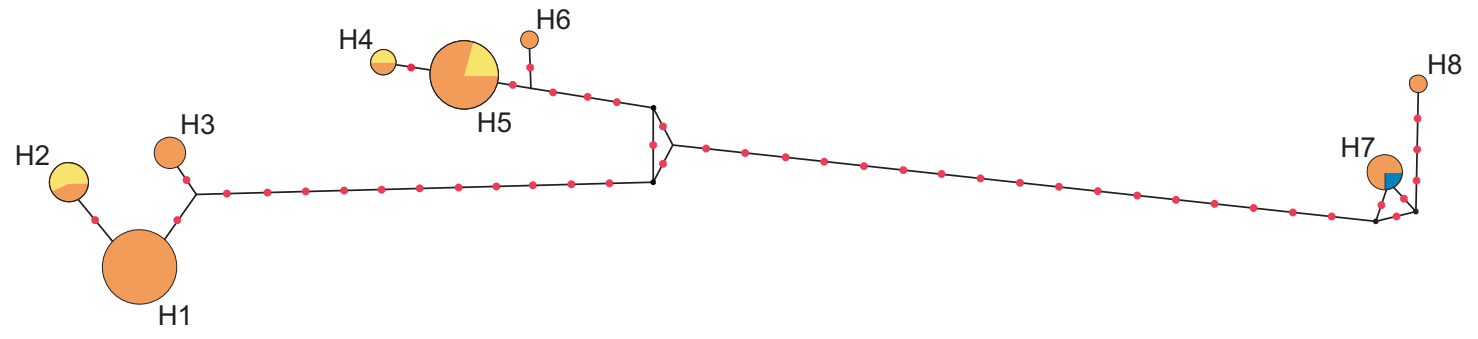
1 substitution



	G2	G3
G1	17 bp	31 bp
G2		23 bp

b Areas

- Bransfield Strait
- Weddell Sea
- Drake Passage



c Stations

- 163-9
- 204-2
- 220-2
- 224-3
- 227-2
- 164-4
- 197-5
- 198-5
- 162-7
- 116-9
- 234-5

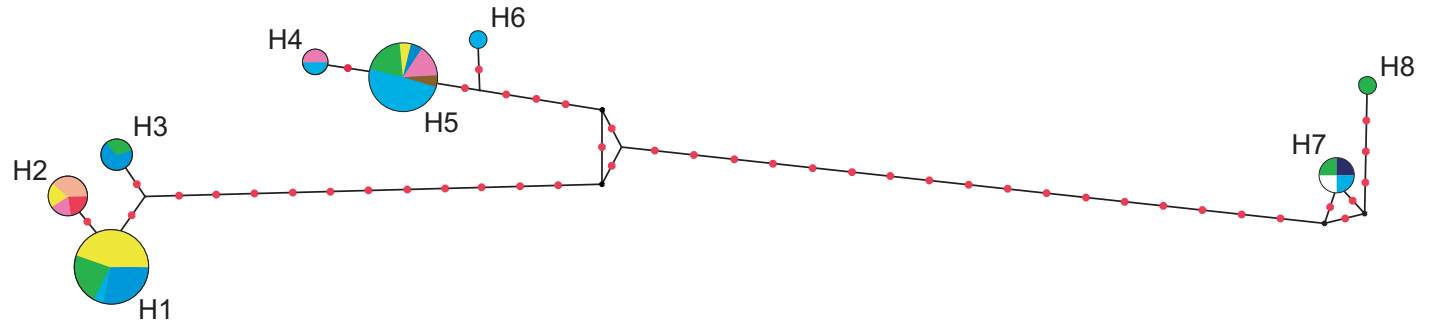
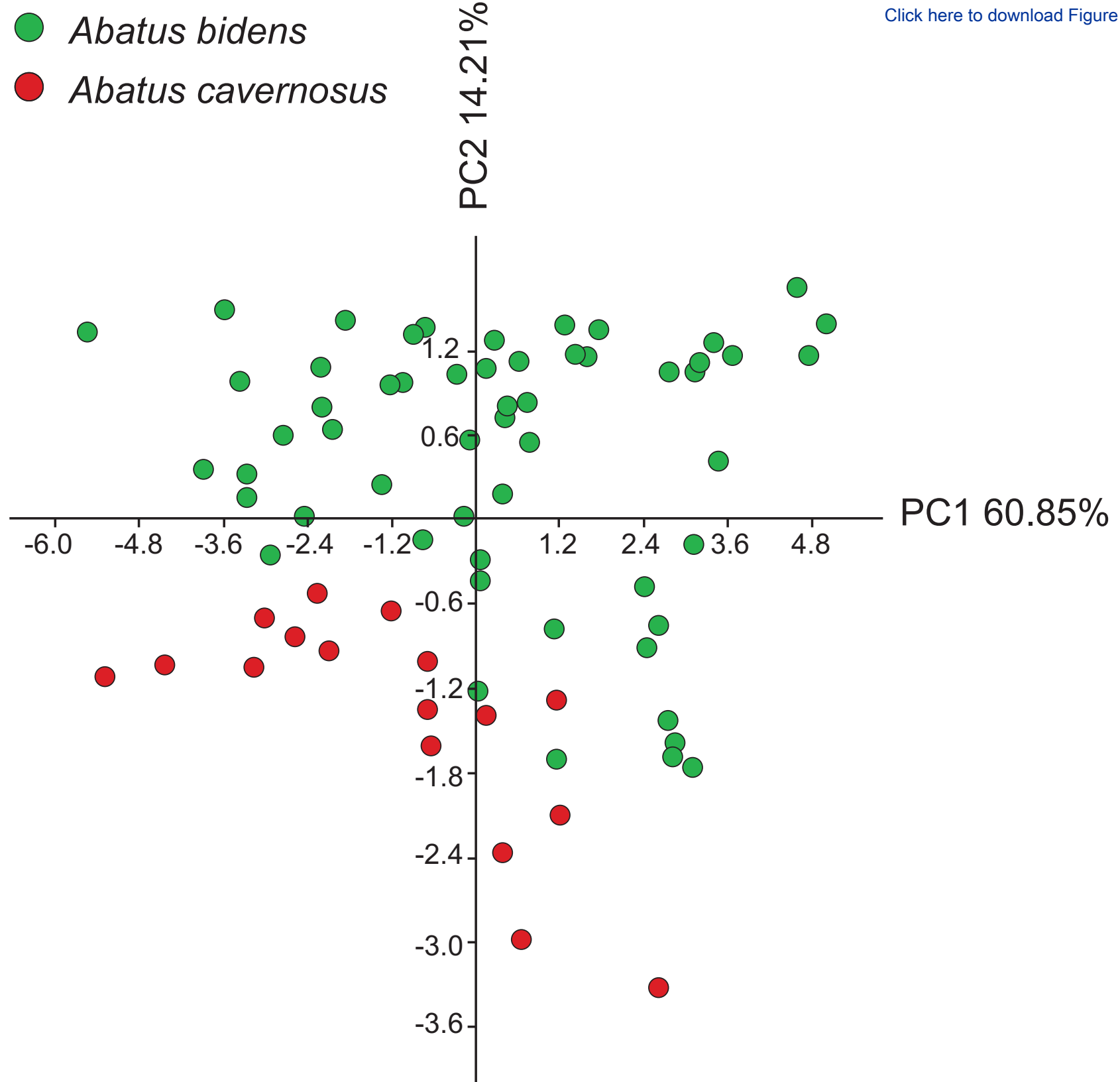


Figure 4



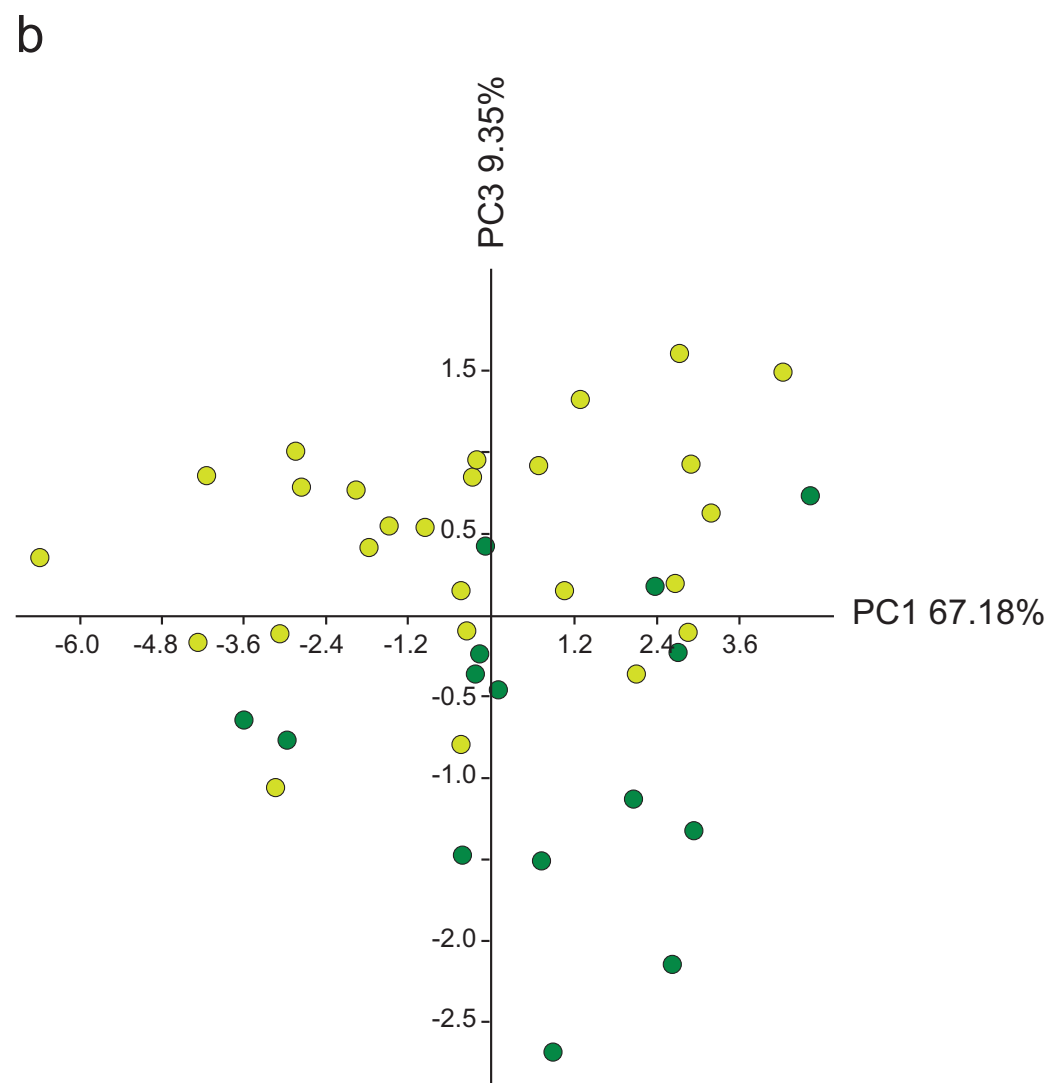
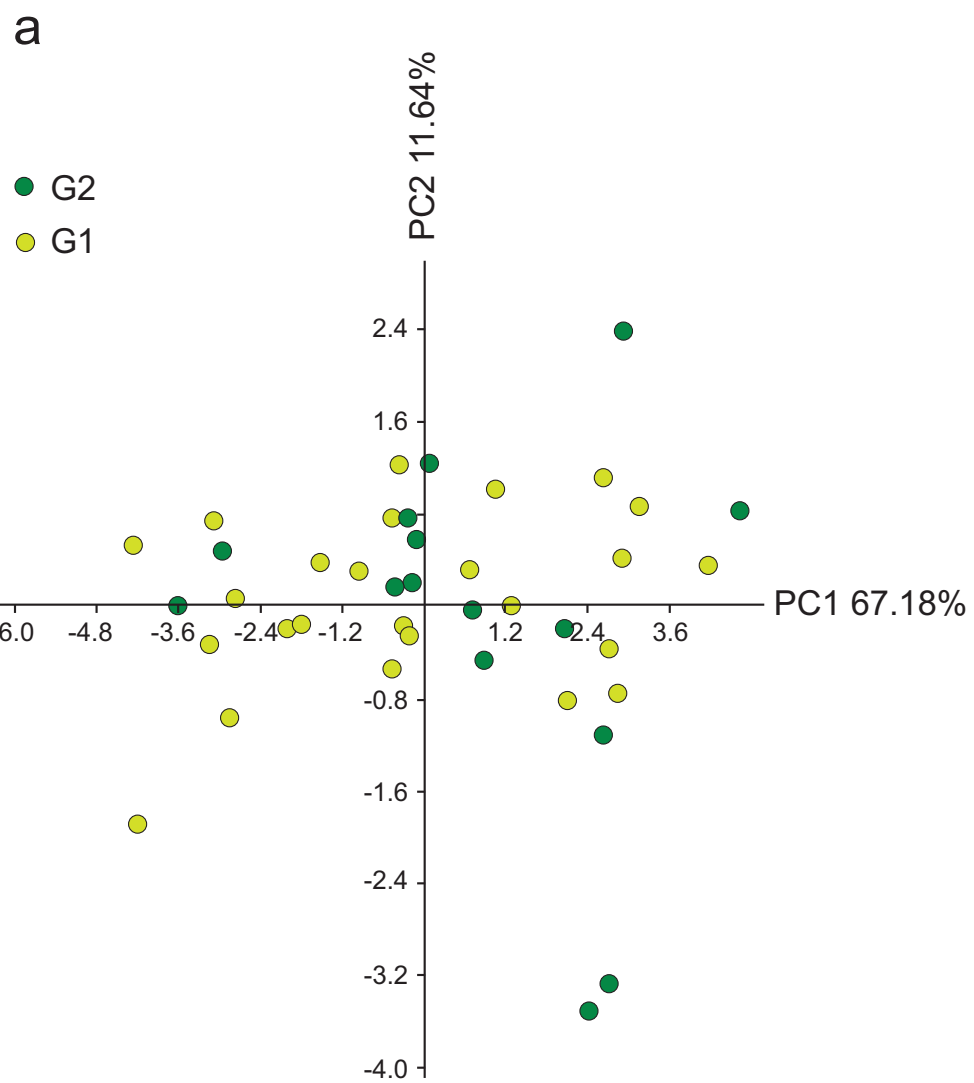


Figure 6

